

## Mn-Cu Based Coating on Graphite Cycling in Alkaline and Neutral Electrolytes for Flexible Supercapacitor Applications

Abdulcabbar YAVUZ<sup>1\*</sup>, Hüseyin FAAL<sup>2</sup>

### Keywords

*Flexible Electrode,  
Energy Storage,  
Ionic Liquid,  
Deep Eutectic  
Solvent,  
Potential Window*

**Abstract** – Notable advancements have been made in the advancement of technologies utilizing flexible screens and sensors. However, the progress in the field of flexible energy storage devices has been comparatively restricted. Research on flexible energy storage electrodes is necessary because of the crucial role of flexibility and stretchability in wearable, biomedical, and portable electronic devices. This study examines the electrochemical characteristics of graphite filaments covered with alloy which possesses flexibility. Electrochemical synthesis of Mn-Cu-based modified graphite was achieved using a deep eutectic solvent at varying static voltages. Analyzed in this study was the electrochemical deposition performance of films in Ethaline deep eutectic solvent, as well as the subsequent cycling of the resultant electrodes in a KOH, Na<sub>2</sub>SO<sub>4</sub> and the mixture of KOH and Na<sub>2</sub>SO<sub>4</sub> electrolytes. The potential window used for this analysis was increased to 1.5 V. The graphite substrate, coated with Mn-Cu through the application of a voltage of -1.9 V, exhibited a length capacitance of 109 mF cm<sup>-2</sup> when cycling electrolyte is the mixture of KOH and Na<sub>2</sub>SO<sub>4</sub>. The film exhibited extensive surface covering and showed promise for utilization in energy storage applications.


### 1. Introduction

As we approach the end of the first quarter of the twenty-first century, it is obvious that the increase in energy and electricity consumption has produced a serious issue. Rapid population increase and changing consumer habits are the two main causes of this global problem because a rapid population could spend more energy. Additionally, daily life in many countries has been changed due to technological improvement. Almost all technological devices (mobile phones, computers, electric vehicles, household goods, etc.) are based on energy consumption. A sizeable amount of the total energy consumption is jointly accounted for by the industrial, transportation, and construction sectors. Global energy demand could be anticipated to double by 2050 and triple by the end of the century. Increasing the efficiency of the current traditional energy systems alone might not be sufficient to meet this demand sustainably (Guney and Tepe, 2017; Mitali et al., 2022).

It seems that conventional energy sources have harmful environmental effects that lead to ecological problems such as acid rain, ground-level ozone production, air and water pollution, global warming, and ozone layer depletion. The quick depletion of available fossil fuel resources has also compelled energy supply firms around the world to think about ways to increase the efficiency and economy of the use of current energy sources, as well as to take action to develop new energy resources. Renewable energy sources were created as a result of overcoming these difficulties and improving the sustainability of energy storage techniques, and they offer significant advantages both economically and environmentally (Hannan et al., 2021; Yang et al., 2018).

In terms of energy usage and power management, energy storage technologies are crucial. It contributes to a sustainable, safe, and clean way of future energy needs. There are numerous techniques for energy storage

<sup>1\*</sup>**Corresponding Author.** Gaziantep University, Faculty of Engineering, Department of Metallurgical and Materials Engineering, Sehitkamil, 27310 Gaziantep, Turkey. E-mail: [ayavuz@gantep.edu.tr](mailto:ayavuz@gantep.edu.tr)  ORCID: 0000-0002-7216-0586

<sup>2</sup>Gaziantep University, Graduate School of Natural and Applied Sciences, Materials Science and Engineering, Sehitkamil, 27310 Gaziantep, Turkey. E-mail: [faal720@gmail.com](mailto:faal720@gmail.com)  ORCID: 0009-0004-7171-8308

**Citation:** Yavuz, A. and Faal, H. (2024). Mn-Cu based coating on graphite cycling in alkaline and neutral electrolytes for flexible supercapacitor applications. *Natural Sciences and Engineering Bulletin*, 1(2), 1-16.

including capacitors and supercapacitors (Luo et al., 2015; Sharma et al., 2019); sodium-sulfur (NaS), lithium-ion, nickel-cadmium (Ni-Cd) and lead-acid batteries (Kalhammer and Schneider, 1976); fuel cells, mechanically pumped hydropower (Luo et al., 2015), compressed air energy storage systems (CAES), and flywheels. Supercapacitor technologies with fast charge-discharge capabilities have become increasingly prominent as a case of the need for high-power applications, maintaining energy quality, and satisfying continuous energy demand (Ho et al., 2010). They have the potential to serve as a more eco-friendly form of energy storage, as they generally contain fewer chemicals that are harmful to the environment and can be recycled. However, it is important to note that while they may reduce the presence of toxic substances, this does not entirely eliminate the possibility of such chemicals being present in certain formulations (Wen et al., 2015). Supercapacitors might, therefore, be crucial components of energy storage systems in the future (González et al., 2016). Some supercapacitors are based on the principle of electrostatic storage, which is achieved by applying a voltage between two electrodes. These kinds of supercapacitors are referred to as electric double-layer capacitors (EDLC). Energy could be stored through an electrolyte solution between two solid electrolytes. Pseudocapacitors and hybrid supercapacitors (their details are given in Section 2) are other main categories of supercapacitors within the context of energy storage techniques (Li et al., 2008).

Electric double-layer capacitors (EDLCs) improve storage capacities by increasing electrical conductivity, increasing the surface area of the electrodes, and reducing pore size (Arumugam et al., 2023). Pseudocapacitors store energy by reversible multi-electron redox faradaic reactions (Sahin et al., 2020). Pseudocapacitors could have higher specific capacitance values, while EDLCs generally exhibit greater cyclic stability and superior power density and energy density performance. As the name implies, hybrid systems also give the option of combining the power source of a capacitor-like electrode (EDLC structure) with the energy source of a battery-like electrode (pseudocapacitor) in the same cell (Iro et al., 2016). The EDLC generally consist of carbon-based materials. The materials of pseudocapacitors are hydroxide, sulphide and oxide-based metals/alloys such as Mn (Mohanty et al., 2023) and Cu (Sayyed et al., 2023). Additionally, conducting polymers are also the material of pseudocapacitors. When different materials belonging to EDLC and pseudocapacitors are combined, hybrid supercapacitors can be obtained.

The main components with a significant impact on the performance of supercapacitors are electrodes and electrolytes (Yavuz et al., 2022). The elements that store and release this energy are identified as electrodes (Baig et al., 2023). Electrolytes are defined as those that provide energy storage and release processes at the interface and facilitate the movement of ions. Therefore, the selection of the correct electrolyte and electrode is important for supercapacitors' performance and efficiency (Iro et al., 2016). Therefore, we have focused on the combination of both electrodes and electrolytes in this study.

The material, structure, conductivity, surface area and electrochemical properties of the electrode are critical factors that influence the electrode's selection. For instance, a combination of EDLC and pseudocapacitive materials could be fabricated for high-performance supercapacitors. In this study, active alloy-coated flexible graphite electrodes have been studied to analyse supercapacitor performance. These coatings could create a larger surface area of the electrode and increase the interaction with the electrolyte. Thus, electrode selection could increase the energy storage capacity by enabling more interaction on the electrolyte interface of the electrodes (Arumugam et al., 2023).

Deep eutectic solvents (DESs) and ionic liquids (ILs) have shared characteristics, such as being liquid at very low temperatures and exhibiting little volatility; they are classified as separate categories of solutions. Ionic liquids are purely ionic compounds, usually consisting of a sizable organic cation and an inorganic or organic anion. Deep eutectic solvents are created by the interaction of a hydrogen bond donor and a hydrogen bond acceptor. This often leads to the formation of a mixture consisting of a quaternary ammonium salt and a hydrogen bond donor, such as urea or aromatic acid. By causing a depression in the melting point, this interaction results in the formation of a eutectic mixture. Contrary to ILs, DESs are not completely ionic and are, hence, more convenient and cost-effective to manufacture. Various electrolytes such as DESs, sodium sulfate ( $\text{Na}_2\text{SO}_4$ ) (Purushothaman et al., 2012), potassium hydroxide (KOH) (Brisse et al., 2018), a mixture of sodium sulfate + potassium hydroxide ( $\text{Na}_2\text{SO}_4 + \text{KOH}$ ) (HCl) (Niknam et al., 2022) and hydrochloric acid could be used for electrodeposition and cycling of electrodes.

The main aim of the study is to analyze the interactions between selected electrodes and electrolytes and how their variations could influence supercapacitor performance. This could be used for the development and optimization of supercapacitor technology. In this research, electrodes, electrolytes, and the interactions between these two components were investigated. The resulting data could be used to evaluate the parameters affecting supercapacitor properties. This research could contribute to our understanding of how these electrolytes and electrodes could affect supercapacitor performance. Mn-Cu-based electrodes were electrodeposited on the graphite layer. After the coating process, modified electrodes were transferred to various electrolytes such as sodium sulfate ( $\text{Na}_2\text{SO}_4$ ), potassium hydroxide (KOH), sodium sulfate and potassium hydroxide mixture ( $\text{Na}_2\text{SO}_4 + \text{KOH}$ ) and hydrochloric acid (HCl) in order to compare their electrochemical performance. This study is the first to electrodeposit Mn-Cu alloy onto a graphite layer using a deep eutectic solvent. Furthermore, it is the first to investigate the electrochemical performance of this alloy in various electrolytes, including alkaline, acidic, and neutral solutions, with a particular focus on the novel  $\text{Na}_2\text{SO}_4 + \text{KOH}$  mixture.

## 2. Materials and Methods

A solution of Ethaline deep eutectic solvent was created by combining two parts ethylene glycol with one part choline chloride, then heating the mixture at a temperature of  $65^\circ\text{C}$  for a duration of 45 minutes. A solution containing 0.5 M  $\text{MnCl}_2$  and 0.5 M  $\text{CuCl}_2$  was produced using an Ethaline deep eutectic solvent. Due to the rapid solubility of both metal chlorides in Ethaline deep eutectic solvent, the mixing duration was limited to a short period of time (usually 10 minutes). A solution was prepared by combining equal quantities of 1 M  $\text{MnCl}_2$  and 1 M  $\text{CuCl}_2$  in a glass beaker at a temperature of  $65^\circ\text{C}$ . The resulting solution contained 0.5 M  $\text{MnCl}_2$  and 0.5 M  $\text{CuCl}_2$ . The graphite electrodes were directly submerged in Ethaline in order to electrodeposit Mn-Cu alloys. No pretreatment step was applied. Cyclic voltammogram curves were generated for the deposition baths containing pure Ethaline, Ethaline with  $\text{Mn}^{2+}$  ions, and Ethaline with  $\text{Cu}^{2+}$  ions. These curves were used to analyze the electrochemical deposition behaviour of pure Ethaline, Mn, Cu, and Mn-Cu in Ethaline on graphite electrodes. Three distinct static voltages (-1.6 V, -1.9 V, and -2.2 V) were individually supplied to the graphite electrodes for a duration of 300 seconds at a temperature of  $65^\circ\text{C}$  in order to produce the alloys.

A three-electrode system was used for the growth and electrochemical characterisation of the electrodes. The reference electrode containing an AgCl layer covered on Ag wire and a saturated potassium chloride electrolyte in a glass body is used in aqueous solutions. In deep eutectic solvents (DESSs), a silver wire is used as a direct reference electrode. The counter electrode was titanium-coated ruthenium mesh. Graphite-coated tape was used as a working electrode. The potentiostat was controlled using a VersaSTAT 3, Princeton Applied Research model potentiostat manufactured by AMATEK Company (USA). The list of chemicals utilized to produce the findings in this study is manganese (II) chloride dihydrate ( $\text{MnCl}_2 \cdot 2\text{H}_2\text{O}$ , >99, Merck), copper (II) chloride dihydrate ( $\text{CuCl}_2 \cdot 2\text{H}_2\text{O}$ , >99, Merck), choline chloride ( $\text{HOC}_2\text{H}_2\text{N}(\text{CH}_3)_3\text{Cl}$ , >99, Alfa Aesar), mono ethylene glycol, >99, Nebioğlu), potassium hydroxide (KOH, >90, Tekkim), sodium sulfate ( $\text{Na}_2\text{SO}_4$ , >90, Merck).

The preparation of the graphite-coated flexible tape electrode is presented in Figure 1. The first step in cleaning the surface of the bulk graphite substrate is to carefully wipe the main graphite surface from which the samples will be taken with a clean napkin. This process ensures that any visible dirt, dust, or debris on the surface is removed (Figure 1a). After the cleaning process is completed, 600 mesh sandpaper is used to make the surface smoother. At this stage, the graphite surface is carefully sandpapered until it has a flat structure like a transom. In this way, the substrate surface gains a smooth and homogeneous structure (Figure 1b). After the sanding process, the graphite surface reaches a clean and flat structure. Now, for basic processing, transparent tape is used to cover the substrate surface and prepare it for further processing. This tape is carefully placed on the graphite surface, and the taping process is performed (Figure 1c). The tape is adhered to the graphite surface by pressing lightly. This pre-bonding step ensures that the tape adheres properly to the surface. The tape is well adhered to the graphite surface. This step ensures that the tape adheres more firmly to the surface and eliminates possible air bubbles. Finally, the tape is completely adhered to the graphite surface, leaving no loose edges or gaps. This step allows the tape to form a tight bond with the graphite surface (Figure 1d). As a result of the banding process, the graphite surface is covered with tape, and a flexible graphite film is formed. This flexible graphite film is removed from the graphite surface to obtain a thin, flexible substrate (Figure 1e & 1f). The samples are prepared

by measuring and cutting the flexible graphite-coated tape (Figure 1g) to the desired size (1 cm<sup>2</sup>). These samples have been used as current collectors (Figure 1h & 1i).

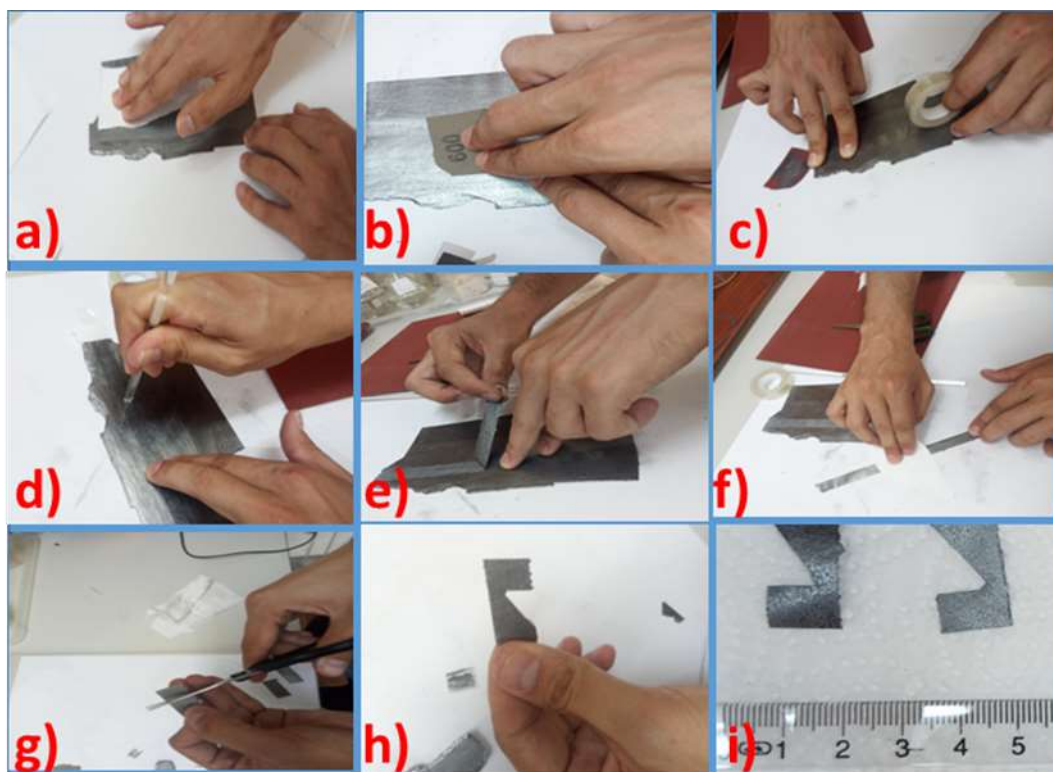


**Figure 1.** Photographs showing the preparation of flexible tape graphite substrate; a) Cleaning the surface of the graphite; b) Sandpapering the surface of the graphite; c) Covering the substrate surface with a tape; d) Adhered to the graphite surface by pressing lightly with glass rod; e) Removing thin flexible graphite film from the graphite surface; f) Homogenising the surface of the graphite tape; g) Cutting the flexible graphite tape; h) Obtaining a graphite film sample of 1 cm<sup>2</sup> size; i) The obtained samples are preserved for the electrode coating test steps after quality standard control.

Once all the sodium sulfate (Na<sub>2</sub>SO<sub>4</sub>) or potassium hydroxide (KOH) were completely dissolved in the water, 1 M Na<sub>2</sub>SO<sub>4</sub> and 1 M KOH solutions were obtained. As a final step, the equal volumes of these two solutions were mixed in a new beaker, resulting in an electrolyte solution consisting of 0.5 M KOH + 0.5 M Na<sub>2</sub>SO<sub>4</sub>. This meticulously prepared electrolyte solution was then ready for use in the experimental procedures. The modified electrodes were then submerged in solutions containing potassium hydroxide (KOH) and sodium sulfate (Na<sub>2</sub>SO<sub>4</sub>), as well as solutions containing combinations of these two electrolytes in equal amounts, to reveal their electrochemical behaviours. By utilizing chronocoulometric, chronoamperometric, cyclic voltammetric, and cyclic polarisation techniques, the electrochemical properties of both pure graphite and coated graphite electrodes were examined. These attributes included capacitance calculations, stability, energy storage capabilities, and rate-limiting reactions.

### 3. Results and Discussion

#### 3.1. Growth of electrodes

The chronocoulometric analysis method was used to apply -1.6 V, -1.9 V, and -2.2 V potentials to graphite-based samples in an Ethaline solution containing 0.5 M MnCl<sub>2</sub> + CuCl<sub>2</sub> at 60 °C for 150 seconds. This allowed us to determine the growth of manganese and copper alloys by electrochemical deposition on the graphite electrode. The red line in Figure 2a is the cyclic voltammogram responses of graphite in Ethaline, including Cu<sup>2+</sup> ions. Oxidation and reduction of copper are observed at around -0.5 V. Redox reactions of Mn<sup>2+</sup> in the electrolyte have been observed (see green line of Figure 2a) with the reduction of Mn starting at around -1.5 V, which could be associated with the initial stages of Mn deposition and growth. These peaks do not belong to the

graphite electrode as the black line in Figure 2b, which is a cyclic voltammogram of graphite in pure Ethaline, does not illustrate redox peaks. Oxidation and reduction peaks of Ethaline having both ions ( $\text{Cu}^{2+}$  and  $\text{Mn}^{2+}$ ) appear (see blue line in Figure 2b). The application of a potential less than 1.5 V could cause the growth of Mn-Cu alloy. The growth of a manganese and copper alloy on a graphite electrode over 150 seconds at potentials of -1.6 V, -1.9 V, and -2.2 V, as well as the alloy's capacity and charging period. The electrochemical plating procedure can be optimized using this data to produce the optimum manganese copper alloy for graphite electrodes. Chronocoulometric results were obtained by the integration of chronoamperometry data.

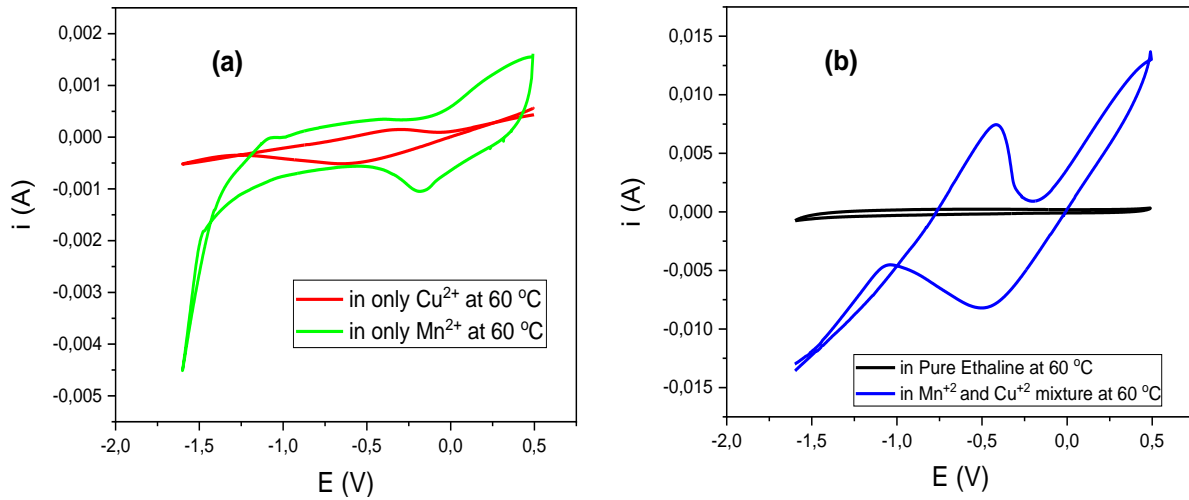


**Figure 2.** Cyclic voltammogram results of bare graphite in a) Ethaline having  $\text{CuCl}_2$  (red line) and Ethaline having  $\text{MnCl}_2$  (red line) and b) pure Ethaline (black line) and Ethaline having both  $\text{CuCl}_2$  and  $\text{MnCl}_2$  (blue line). The scan rate and temperature of the experiments are  $50 \text{ mV s}^{-1}$  and  $60 \text{ }^\circ\text{C}$ .

The chronoamperometry method was employed for electrodeposition of manganese and copper metals onto graphite tapes (Figure 3a). Chronocoulometric data of the electrochemical deposition of a manganese-copper-based layer on the graphite electrode in Figure 3b. The charge change will be, accordingly, a stabilized line over time if the current flux approaches a constant value with time. This shows that the electrochemical reaction has reached equilibrium, and the current is stable.

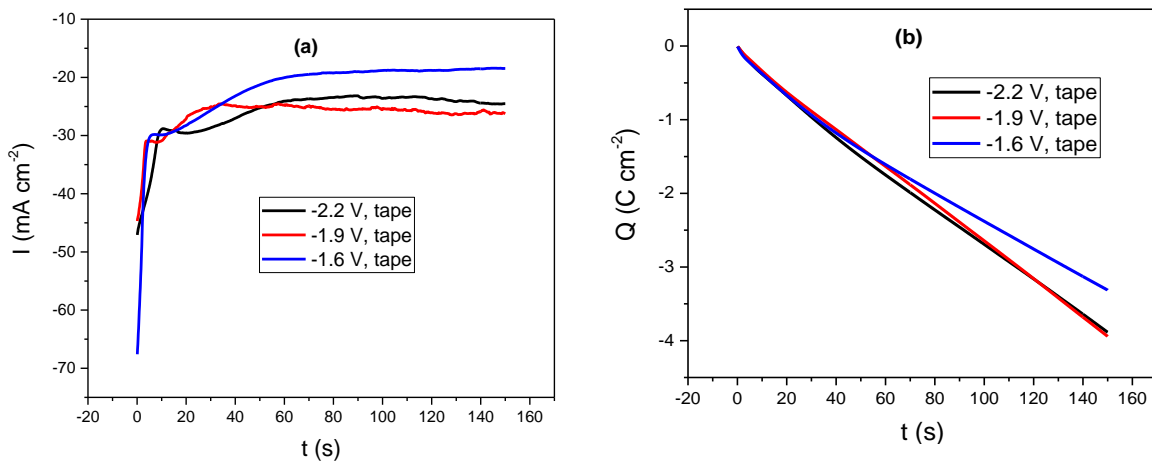


**Figure 3.** The chronoamperometry and chronocoulometry responses of Mn-Cu growth at  $60 \text{ }^\circ\text{C}$  for 150 seconds a) chronoamperometry data of Mn-Cu alloy growth on graphite coated tape by application of -2.2 V (black line), -1.9 V (red line) and -1.6 V (blue line), and b) chronocoulometry data of the growth given in panel a.

It is known that the current graph expresses the change in the amount of charge (coulomb) carried in a certain time. For this reason, over time, a constant current results in a steady build-up of charge. When the current is high, the charge accumulation starts quickly and then increases more quickly over time. This indicates that the electrochemical process is proceeding steadily and that the current does not change with time.

### 3.2. Electrochemical Characterisation of the Electrodes

#### 3.2.1. Mn-Cu electrodeposited by application of -1.6 V

In the initial stage, graphite surfaces were coated with Mn-Cu films under a constant potential of -1.6 V using a solution containing 0.5 M  $Mn^{+2}$  and 0.5 M  $Cu^{+2}$  ions in Ethaline. This process enabled the deposition of metal alloys onto the graphite surfaces. Then, the electrodes were immersed in different electrolyte liquids determined as 1 M  $Na_2SO_4$  and 1 M HCl in the range of -1 to 0.5 V with the same scanning rate. Cyclic voltammetry tests were performed at the same scanning rate to examine their electrochemical behaviour. Upon evaluating the results of the cyclic voltammetry tests, as depicted in Figure 4a and 4c, the current density in the HCl-based electrolyte decreases upon cycling and reduction-oxidation peaks become stable after tens of cycling, and current ranged from  $-0.5 \text{ mA cm}^{-2}$  to  $+0.5 \text{ mA cm}^{-2}$ . Additionally, in the  $Na_2SO_4$  electrolyte, this value corresponds to peaks within the range of  $-4 \text{ mA cm}^{-2}$  to  $+1 \text{ mA cm}^{-2}$ . The current graph is stable, meaning that this electrolyte could be used for cycling in the area of energy storage devices. Moreover, upon reviewing Figure 4b and 4d, it became evident that the cyclic stability of HCl acid was lower compared to that of  $Na_2SO_4$  electrolyte, and cyclic stability did not establish quickly. Therefore, we concluded that HCl acid is not suitable for electrochemical tests.

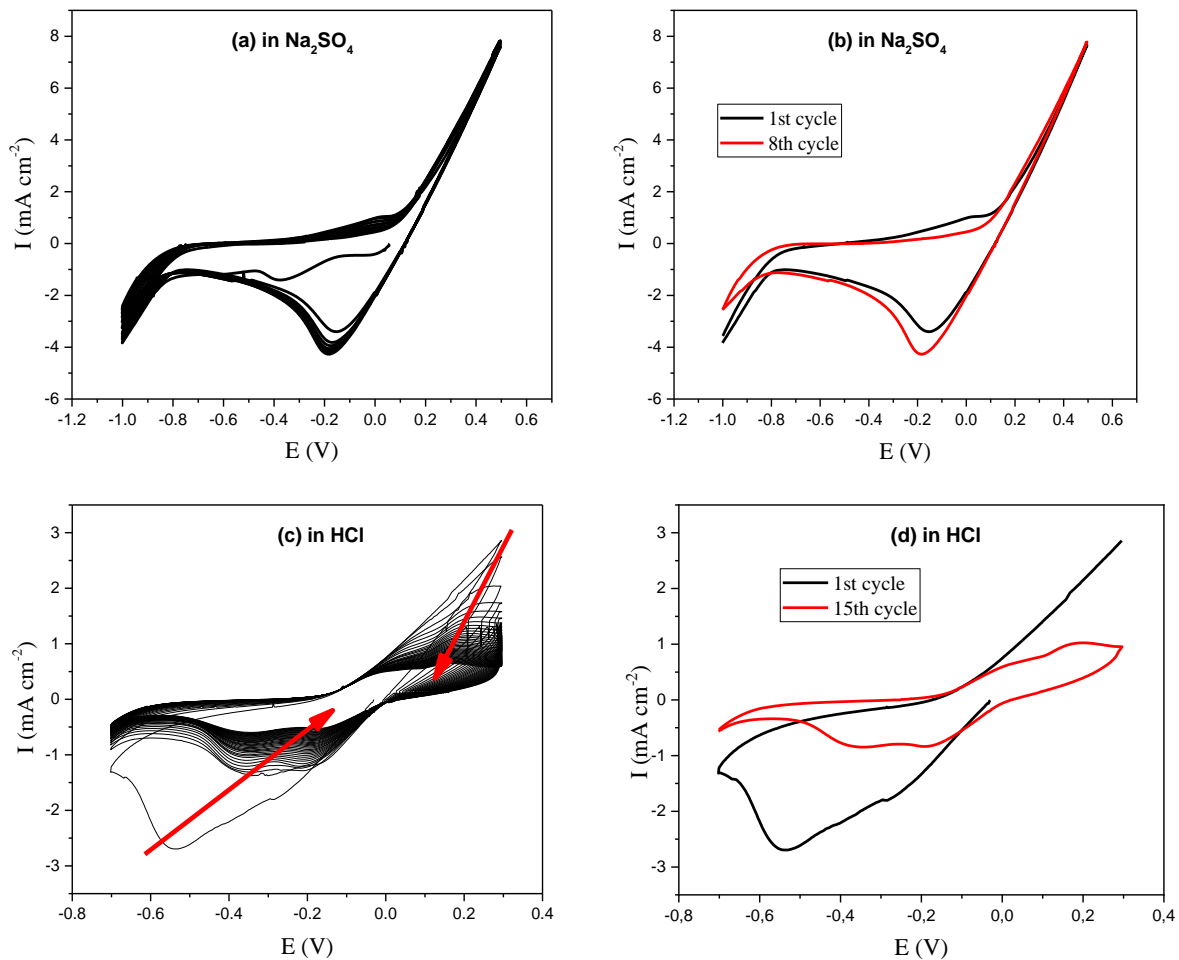


**Figure 4.** a) The cyclic voltammety responses of Mn-Cu alloys cycling in 1 M  $Na_2SO_4$ . b) 1<sup>st</sup> and 8<sup>th</sup> cycle of Mn-Cu alloy in 1 M  $Na_2SO_4$ . c) Cyclic voltammety responses of Mn-Cu alloys cycling in 1 M HCl. d) first and 15<sup>th</sup> cycle of Mn-Cu alloy in 1 M HCl. The electrodes were electrodeposited by application of -1.6 V in Ethaline containing  $Mn^{2+}$  and  $Cu^{2+}$  ions.

Furthermore, with insights gained from the results of cyclic voltammetry tests conducted in various electrolytes, an important role of electrolyte selection in influencing electrochemical properties and energy storage capacity has been discovered. The coating process, which was carried out by applying a potential of -2.2 V to the graphite surfaces by using an Ethaline solution containing 0.5 M  $Mn^{+2}$  and 0.5 M  $Cu^{+2}$ , was completed. Figure 5 illustrates the decrease of current upon cycling. However, the current responses evolve and become stable. Figure 5c illustrates the area under the current-voltage curve of the mixing electrolyte is higher than that of the other electrolyte. Figure 5c confirms that the mixed electrolyte is a more efficient option in terms of charge storage capacity.

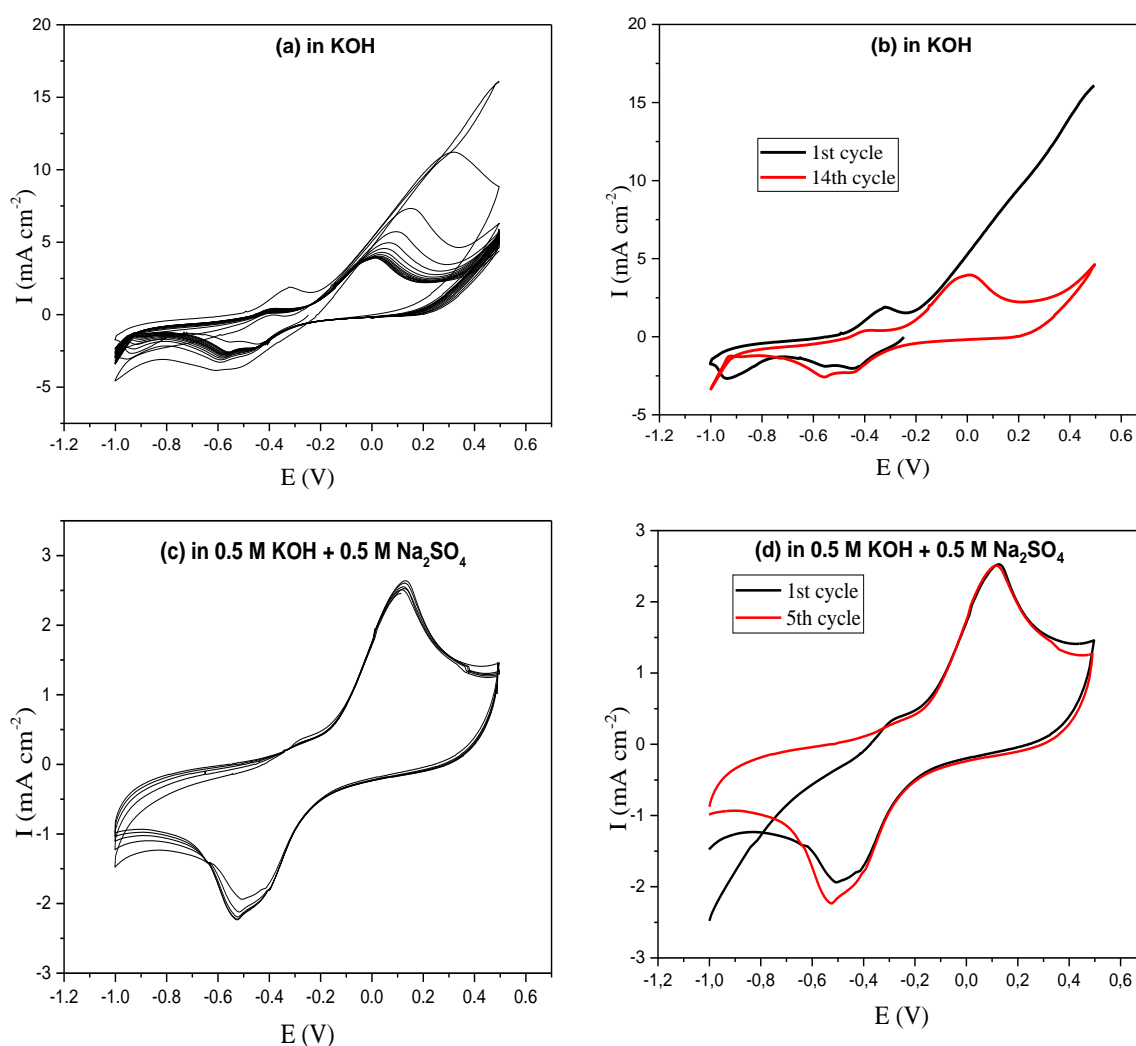
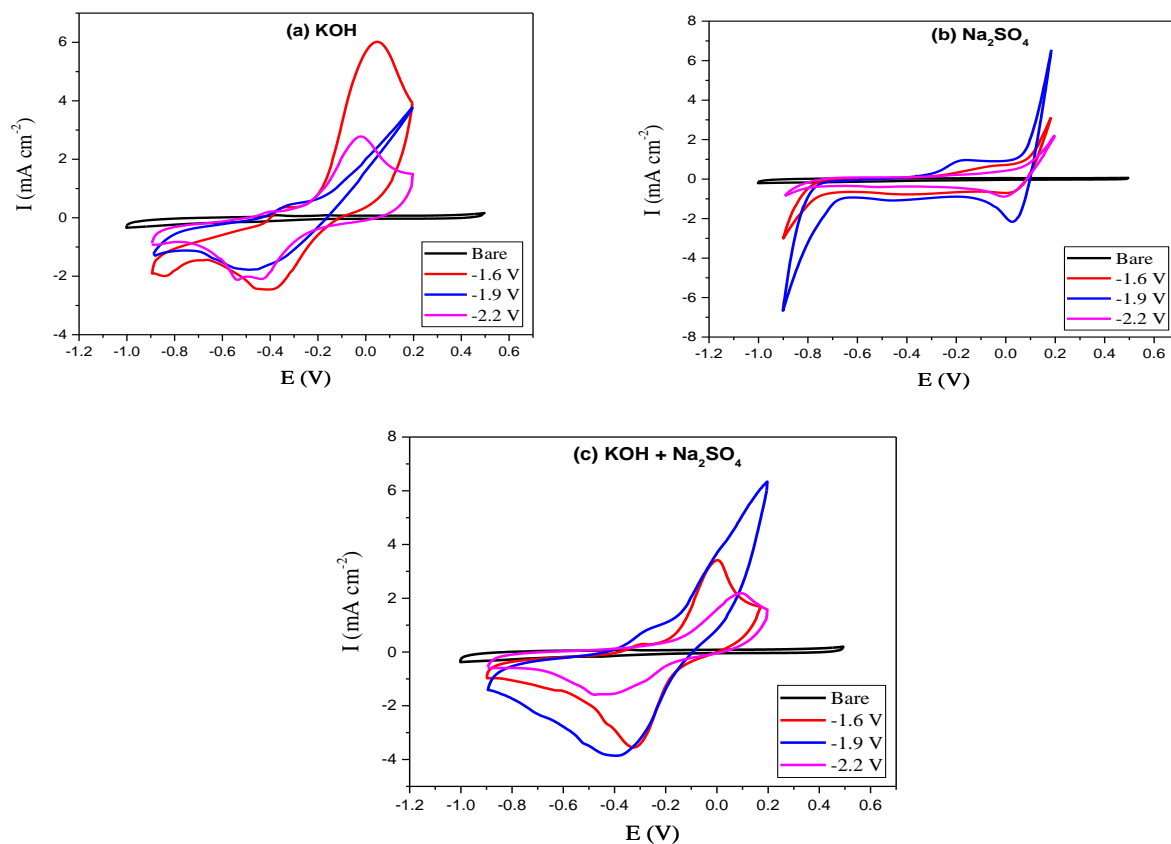


**Figure 5.** a) The cyclic voltammetry responses of Mn-Cu alloys cycling in 1 M KOH. b) 1<sup>st</sup> and 14<sup>th</sup> cycle of Mn-Cu alloy in 1 M KOH. c) cyclic voltammetry responses of Mn-Cu alloys cycling in 0.5 M Na<sub>2</sub>SO<sub>4</sub> + 0.5 M KOH. d) 1<sup>st</sup> and 5<sup>th</sup> cycle of Mn-Cu alloy in 0.5 M Na<sub>2</sub>SO<sub>4</sub> + 0.5 M KOH. The electrodes were electrodeposited by application of -2.2 V in Ethaline containing  $Mn^{2+}$  and  $Cu^{2+}$  ions

A preliminary study was conducted to determine the effects of different solution compositions and voltage levels on the electrochemical performance of Mn-Cu coatings and approach optimal values. In this preliminary study, processes were carried out using different solutions with varying compositions and concentrations, such as KOH, Na<sub>2</sub>SO<sub>4</sub>, and 0.5 M KOH + 0.5 M Na<sub>2</sub>SO<sub>4</sub>, employing three uniform voltage levels (-1.6, -1.9, and -2.2 V) for each solution. In this case, consistent voltage levels were applied for each solution. As a result of these processes, it was observed that the coating had a significant impact on the electrochemical performance of the electrodes (in Figure 6). Particularly, in processes conducted within 1 M KOH, 1 M Na<sub>2</sub>SO<sub>4</sub>, and 0.5 M KOH + 0.5 M Na<sub>2</sub>SO<sub>4</sub>

mixed solutions, it was noted that the different voltage levels (-1.6, -1.9, and -2.2 V) did not yield the same. The cyclic voltammogram responses of the alloy-based coatings were examined by comparing the current values of bare graphite and Mn-Cu coated graphite in the solutions of 1 M KOH, 1 M Na<sub>2</sub>SO<sub>4</sub>, and the mixture of 0.5 M KOH + 0.5 M Na<sub>2</sub>SO<sub>4</sub> in Figure 6. The current value given by bare graphite in three solutions is approximately 0.4 mA (in Figure 6a, b, c). Mn-Cu coated graphite has been observed to provide around 4 mA in 1 M KOH solution (in Figure 6a) and about 6 mA in 1 M Na<sub>2</sub>SO<sub>4</sub> solution (in Figure 6b). However, the current value generated by Mn-Cu coated graphite tapes at a potential of -1.9 V in a mixture of solution of 0.5 M KOH and 0.5 M Na<sub>2</sub>SO<sub>4</sub> was calculated to be around 6.5 mA (in Figure 6c).

As a result of the cyclic voltammogram data, it was observed that the electrochemical performance of Mn-Cu-coated graphite was significantly higher compared to that of bare graphite. In this context, it was determined that the optimal operating voltage was -1.9 V, and it was planned to continue the experiments using three different solvents. These experiments are important steps toward further optimizing the electrochemical performance.



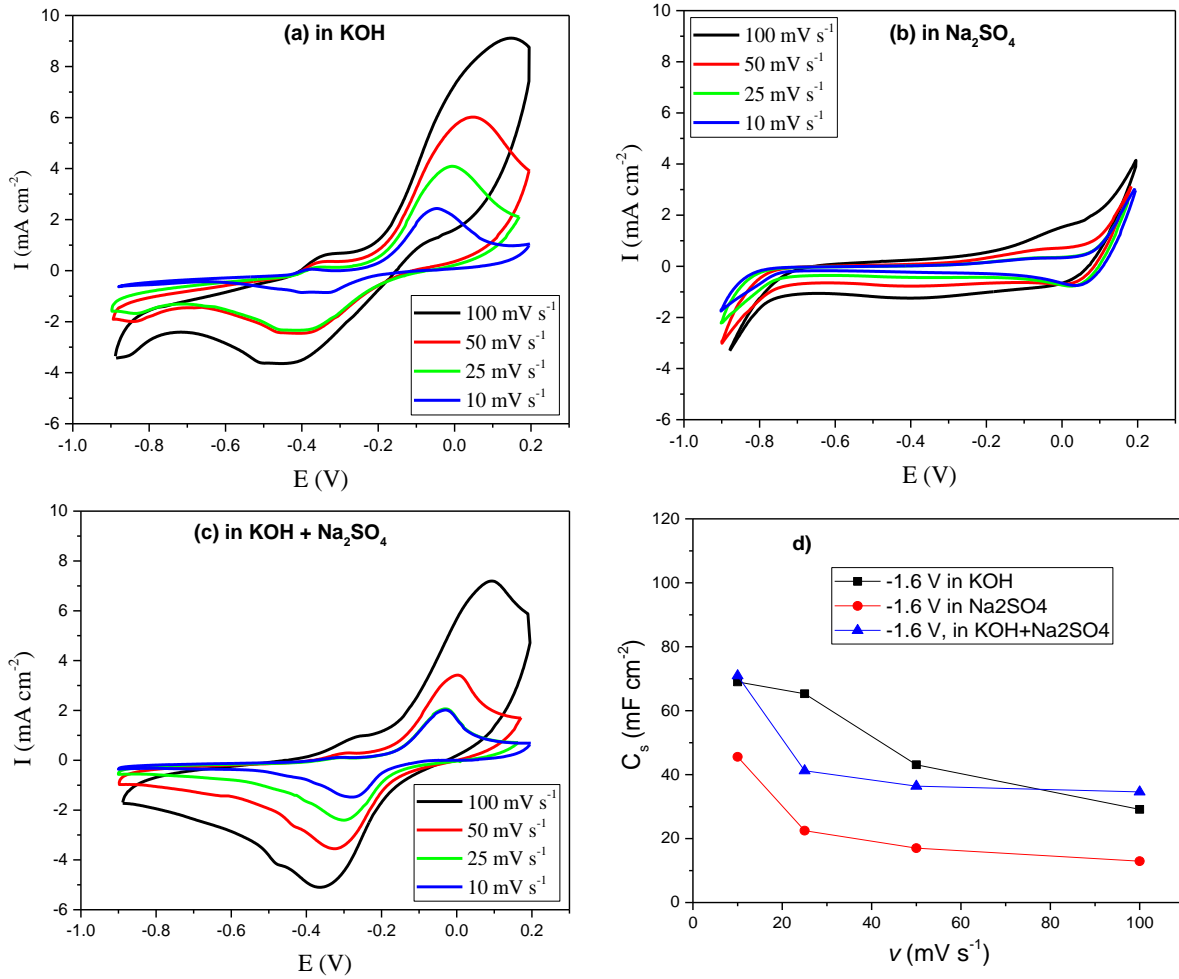
**Figure 6.** The cyclic voltammogram results of all types of graphite films cycled a) in 1 M KOH ( $v = 50 \text{ mV s}^{-1}$ ). b) 1 M Na<sub>2</sub>SO<sub>4</sub> ( $v = 50 \text{ mV s}^{-1}$ ). c) 0.5 M Na<sub>2</sub>SO<sub>4</sub> + 0.5 M KOH ( $v = 50 \text{ mV s}^{-1}$ )

Figure 7 is obtained when the experiment was carried out by taking Mn-Cu coated graphite samples obtained by applying -1.6 V potential using Ethaline. Then, the samples were subjected to cyclic voltammetry experiments in three different electrolyte solutions with electrode potentials ranging from -0.9 V to 0.2 V. Different scan rates (100 mV/s, 50 mV/s, 25 mV/s, and 10 mV/s) were used for these studies.

All graphs in Figure 7 show the increase in the current density of Mn-Cu alloys obtained at different electrode potentials with the increase in scanning speed. These observations explain that the current density in electrochemical reactions is a reflection of the rate of charge transfer. As the scanning speed increases, the amount of charge transfer per unit time increases, increasing current density. The data shown in Figure 7b, however, also show a distinct scenario. Current density maxima are observed in these figures at -3 and 3 mA cm<sup>-2</sup>. Comparatively to Figures 7a and 7c, this figure's area under the curve is noticeably smaller. This implies that



the electrolyte in Figure 7b has less storage capacity and electrochemical capacity than the covered surfaces of the other samples.



**Figure 7.** The cyclic voltammetry data Mn-Cu coated from Ethaline Deep Eutectic Solvent on graphite by application of -1.6 V and now cycling in a) 1 M KOH; b) 1 M Na<sub>2</sub>SO<sub>4</sub> and c) an electrolyte consisting of 0.5 M KOH and 0.5 M Na<sub>2</sub>SO<sub>4</sub>. The scan rates are given in the panels. d) Plot of the area capacitance of the electrodes given in panel a, panel b, and panel c depending on scanning speed.

The specific capacitance ( $C$ ) is generally expressed using the following formula:

$$C = \frac{2}{A \cdot \Delta V} \int \frac{I dV}{v} \quad (1)$$

Where:

- $C$  is the specific capacitance ( $F \text{ cm}^{-2}$ ),
- $I$  represents the current density ( $A \text{ cm}^{-2}$ ),
- $\Delta V$  stands for the potential difference (V),
- $v$  signifies the scan rate ( $\text{mV s}^{-1}$ ),
- $A$  is the area of active materials of the working electrode ( $\text{cm}^2$ )

Specific capacitance refers to the amount of charge stored on an electrode surface during an electrochemical process. The scanning rate, on the other hand, indicates the speed of the electrode potential in voltammetry

experiments. Referring to Figure 7, the relationship between specific capacitance and scan rate is inversely proportional. That is, as the scanning speed increases, the specific capacitance decreases.

**Table 1.** Specific capacitance values of Mn-Cu coated graphite tapes electrodeposited at -1.6 V potential depending on the varying scanning rates in different electrolyte solutions

Scan Rate (mV s <sup>-1</sup> )	Specific Capacitance in KOH (mF cm <sup>-2</sup> )	Specific Capacitance in Na <sub>2</sub> SO <sub>4</sub> (mF cm <sup>-2</sup> )	Specific Capacitance in KOH + Na <sub>2</sub> SO <sub>4</sub> (mF cm <sup>-2</sup> )
100	29	13	35
50	43	17	36
25	65	23	41
10	69	46	71

The same conclusion may be drawn about this by looking at the experimental data in Table 1. At higher scan rates (e.g., 100 mV/s), the measured specific capacitance value in the KOH electrolyte is 29 mF cm<sup>-2</sup>. As the scan rate decreases (e.g., 10 mV/s), the specific capacitance value increases, reaching 69 mF cm<sup>-2</sup>. This indicates that slower scan rates (higher time scale) allow for greater charge storage capacity on the electrode surface. Decreasing the scan rate allows for more charge storage on the electrode surface, leading to higher capacitance values. Moreover, different electrolyte solutions exhibit similar trends, with capacitance values increasing as the scan rate decreases.

### 3.2.2. Mn-Cu electrodeposited by application of -1.9 V

When comparing the graphs in Figure 8 and results in Table 2, a distinct difference in the data obtained from the common electrolytes is observed. For instance, the current density values at a scan rate of 100 mV/s generally range between -2 and 4 mA cm<sup>-2</sup> on average in Figure 8. In the Na<sub>2</sub>SO<sub>4</sub> electrolyte, the current density values vary between -1 and 7 mA cm<sup>-2</sup>. Furthermore, in the 1 M KOH + 1 M Na<sub>2</sub>SO<sub>4</sub> electrolyte, the values span from -4 to 8 mA cm<sup>-2</sup>.

**Table 2.** Specific capacitance values of Mn-Cu coated graphite tapes at -1.9 V potential depending on the varying scanning rates in different electrolyte solutions

Scan Rate (mV s <sup>-1</sup> )	Specific Capacitance (mF cm <sup>-2</sup> ) in KOH	Specific Capacitance (mF cm <sup>-2</sup> ) in Na <sub>2</sub> SO <sub>4</sub>	Specific Capacitance (mF cm <sup>-2</sup> ) in KOH + Na <sub>2</sub> SO <sub>4</sub>
100	12	22	29
50	18	31	50
25	28	42	61
10	43	81	109

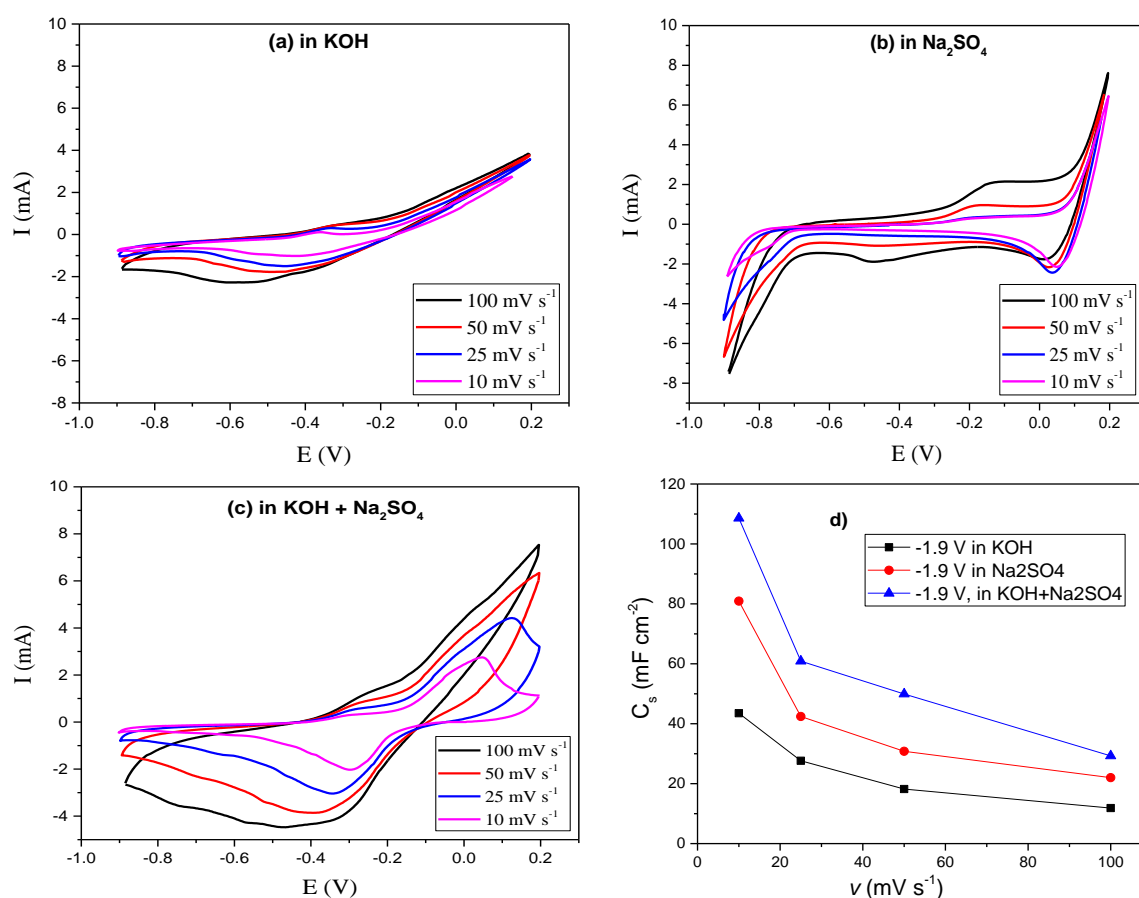


**Figure 8.** The cyclic voltammograms of Mn-Cu alloy in a) 1 M KOH, b) 1 M  $\text{Na}_2\text{SO}_4$  and c) an electrolyte consisting of 0.5 M KOH and 0.5 M  $\text{Na}_2\text{SO}_4$ . Mn-Cu alloy coating on graphite tapes was obtained in Ethaline deep eutectic solvent by applying a constant voltage of -1.9 V. d) Plot of the area capacitance of the electrodes given in panel a, panel b, and panel c depending on scanning speed.

### 3.2.3. Mn-Cu electrodeposited by application of -2.2 V

The photographs of the Mn-Cu coating of graphite are presented in Figure 9. The current density values range from -3 to 4  $\text{mA cm}^{-2}$  in the KOH electrolyte. In the  $\text{Na}_2\text{SO}_4$  electrolyte, these values vary between -1 and 2  $\text{mA cm}^{-2}$ . For the 1 M KOH + 1 M  $\text{Na}_2\text{SO}_4$  electrolyte, the values fall within the range of -2.5 to 3  $\text{mA cm}^{-2}$ . Exploring the factors underlying these discrepancies, we find that at higher scan rates, the time allocated to the redox reaction diminishes, resulting in higher peak current values, especially at higher voltages.

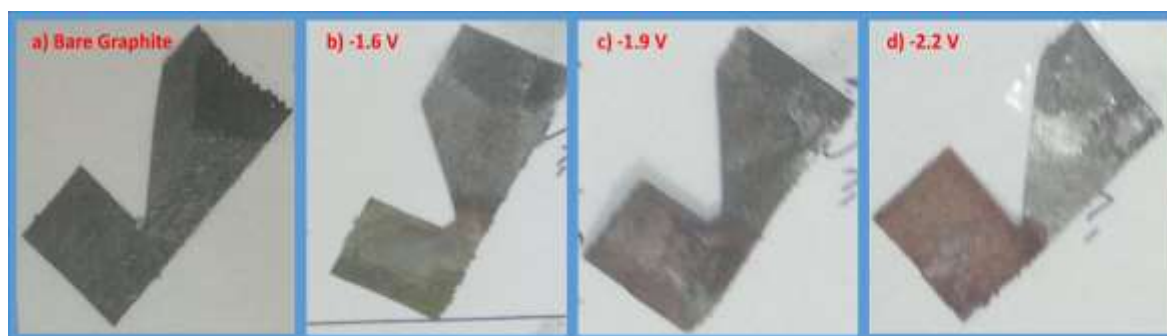


**Figure 9.** Photograph of a) bare graphite; b) Mn-Cu alloy coating on graphite tapes obtained in Ethaline deep eutectic solvent by applying a constant voltage of -1.6V; c) Mn-Cu alloy coating on graphite tapes obtained in Ethaline deep eutectic solvent by applying a constant voltage of -1.9 V; d) Mn-Cu alloy coating on graphite tapes obtained in a deep eutectic solvent by applying a constant voltage of -2.2 V

Additionally, considering the alloy deposition process, we note that lower negative voltage values generally lead to sparser and thinner coating layers (Figure 9). As ions are gradually transported to the surface, the coating layer becomes more irregular and filled with voids. However, at higher negative voltages, denser and more compact coating layers were observed (Figure 9c and 9d). Faster ion transport at higher voltages seems to yield a more homogeneous layer. All these processes, supported by our graphical data, collectively highlight the effects of different voltage levels and scan rates on the electrochemical coating process.

Comparing previous experimental figures by analyzing the graphs of Figure 10, in contrast to what was anticipated under the same scanning speed and electrolyte conditions, the flexible graphite samples coated at higher voltage exhibit lower current peaks. Numerous predictable and unforeseen causes can be responsible for this behaviour, and it might be related to how electro-coating works. Because they carry more energy at higher voltages, the ions in the electrolyte could move to the surface layer more quickly. A more compact and dense coating layer may have occurred as a result. On the other hand, a coating layer may have become thinner and thinner because the ions carry less energy at lower voltages.

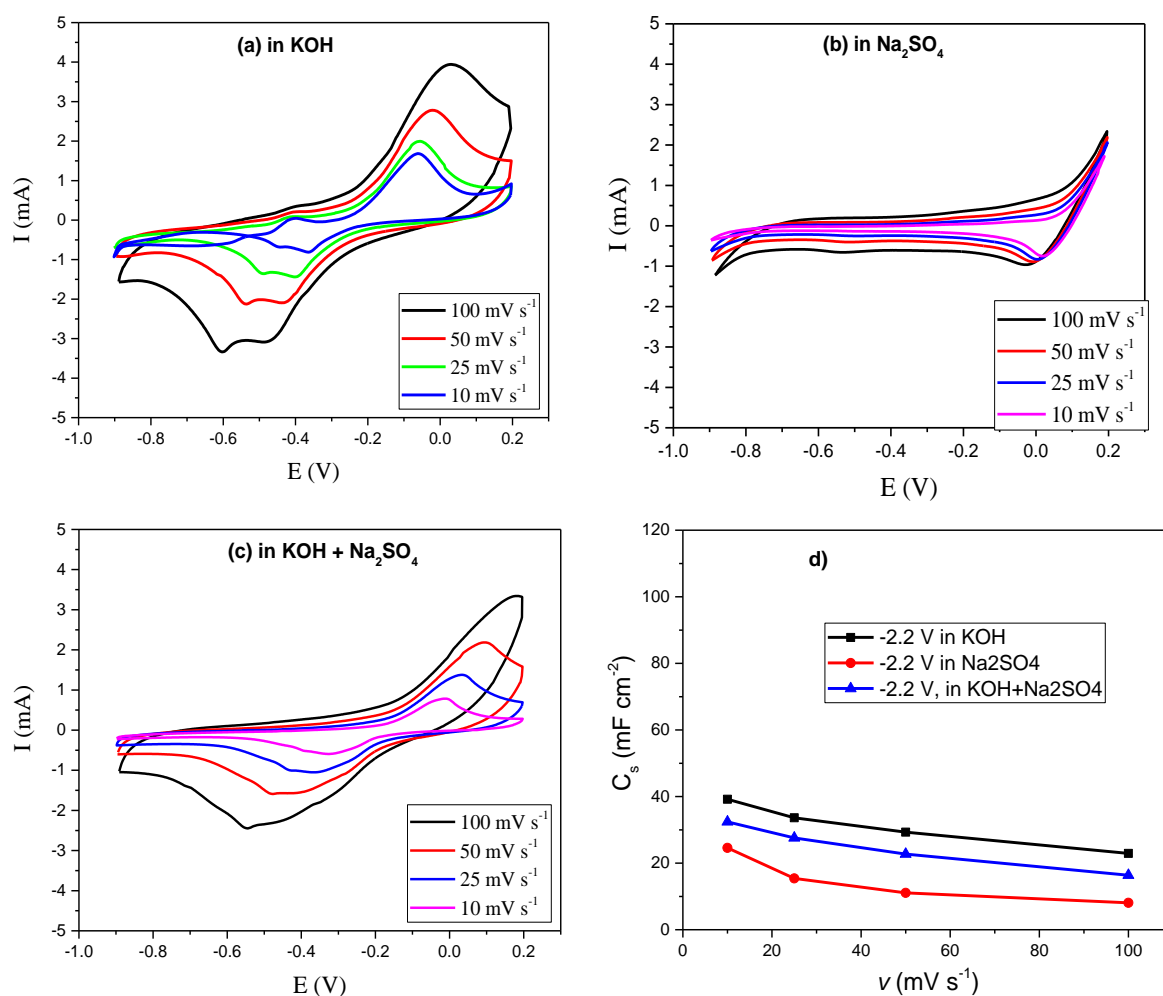


**Figure 10.** The cyclic voltammograms of Mn-Cu alloy in a) 1 M KOH, b) 1 M Na<sub>2</sub>SO<sub>4</sub> and c) an electrolyte consisting of 0.5 M KOH and 0.5 M Na<sub>2</sub>SO<sub>4</sub>. Mn-Cu alloy coating on graphite tapes was obtained in Ethaline deep eutectic solvent by applying a constant voltage of -2.2 V. d) Plot of the areal capacitance of the electrodes given in panel a, panel b, and panel c depending on scanning speed.

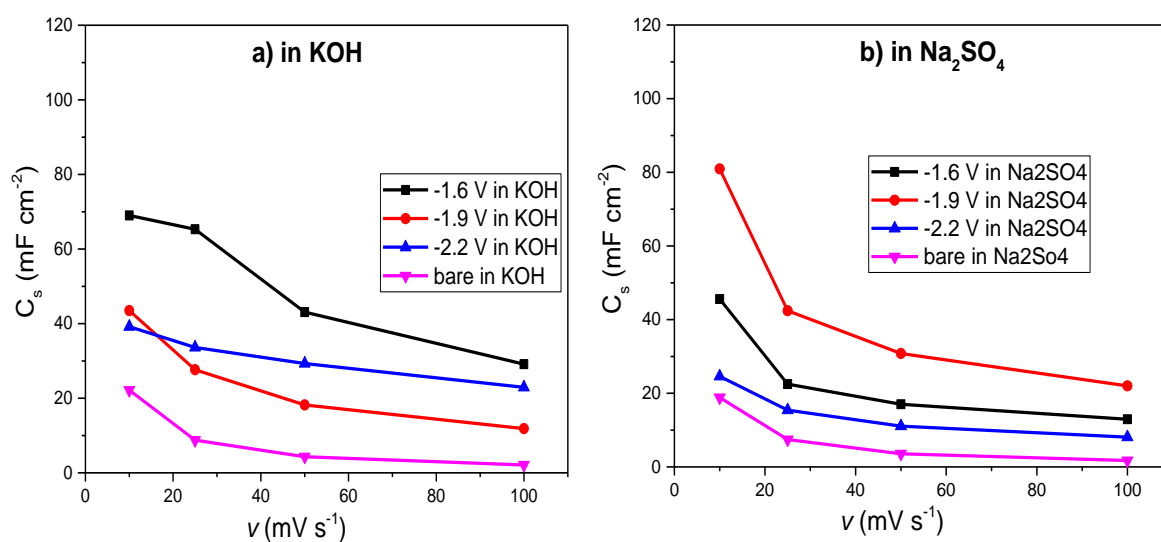
Figure 10 and Table 3 present specific capacitance values obtained at various scanning rates in different electrolyte solutions: KOH, Na<sub>2</sub>SO<sub>4</sub>, and a mixture of KOH + Na<sub>2</sub>SO<sub>4</sub>. These data provide valuable insights into the relationship between electrolyte compositions, scanning rates, and specific capacitance values. Upon examination, a clear trend emerges in the specific capacitance values across the different electrolyte solutions.

**Table 3.** Specific capacitance values of Mn-Cu coated graphite tapes at -2.2 V potential depending on the varying scanning rates in different electrolyte solutions

Scan Rate (mV s <sup>-1</sup> )	Specific Capacitance (mF cm <sup>-2</sup> ) in KOH	Specific Capacitance (mF cm <sup>-2</sup> ) in Na <sub>2</sub> SO <sub>4</sub>	Specific Capacitance (mF cm <sup>-2</sup> ) in KOH + Na <sub>2</sub> SO <sub>4</sub>
100	23	8	16
50	29	11	23
25	34	15	28
10	39	25	32

When examining the graphs in Figure 10 individually, the results obtained under different coating voltages offer valuable insights. Firstly, the KOH electrolyte data acquired at -1.6 V coating voltage greatly outperforms the data obtained at other coating voltages (Figure 10a). These results demonstrate how the electrolyte and the coating voltage of -1.6 V improve and increase the electrode's capacitance properties. Notably, even better results were obtained in comparison to the uncoated graphite-specific capacitance values and the -1.9 V and -2.2 V coatings. This demonstrates the potential of slower scan speeds to accommodate a higher capacity for charge storage on the electrode surface and highlights the critical importance of selecting the right electrolyte.

Analysis of the data acquired under a coating voltage of -1.9 V similarly reveals a tendency similar to the data shown in Figure 11a. The reported specific capacitance value in the KOH electrolyte is 12 mF cm<sup>-2</sup> at higher scan rates (for example, 100 mV/s). The specific capacitance value rises to a maximum of 43 mF cm<sup>-2</sup> when the scan rate falls (for example, to 10 mV/s). When evaluating the results acquired in the Na<sub>2</sub>SO<sub>4</sub> electrolyte under a -1.9 V coating voltage, the same pattern is observed. Higher specific capacitance values are produced when the scan rate is reduced. For instance, the specific capacitance is 22 mF cm<sup>-2</sup> at a scan rate of 100 mV/s but increases to 81 mF cm<sup>-2</sup> with a scan rate of 10 mV/s (Figure 11b).



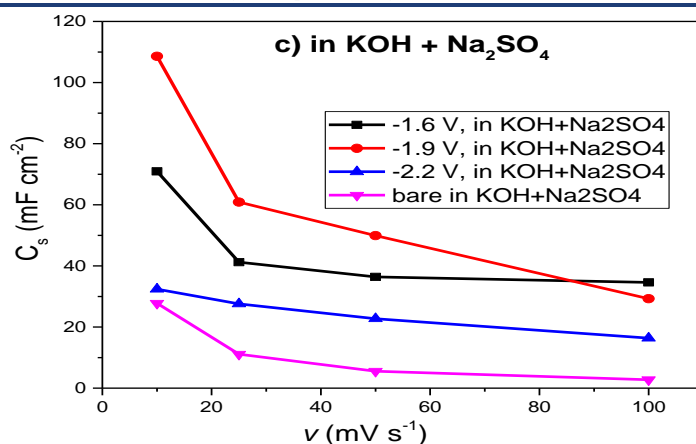


**Figure 11.** Specific capacitance of Mn-Cu based alloy on graphite depending on the applied coating voltage at different values a) cycled in 1 M KOH; b) cycled 1 M Na<sub>2</sub>SO<sub>4</sub> and; c) cycled in the mixture of 0.5 M KOH and 0.5 M Na<sub>2</sub>SO<sub>4</sub> at various scanning speed.

A comparison of the capacitances of metal-based supercapacitor electrodes, as reported in the literature, is provided in Table 4. The study of data obtained using the mixed KOH + Na<sub>2</sub>SO<sub>4</sub> electrolyte also yielded similar results. It is obvious that for scan rate measurements, the best results are obtained with a constant -1.9 V coating voltage. For instance, the specific capacitance value is 29 mF cm<sup>-2</sup> at a scan rate of 100 mV/s, but it increases to 109 mF cm<sup>-2</sup> with a scan rate of 10 mV/s (in Figure 11c).

Additionally, the high capacitance characteristics of the 0.5 M KOH + 0.5 M Na<sub>2</sub>SO<sub>4</sub> concentrated electrolyte are supported by the capacitance values under the -1.6 V coating voltage. These experimental graphs demonstrate, in conclusion, how important electrolyte composition and scan rate are in determining certain capacitance values. The complicated nature of these systems' energy storage mechanisms is underlined by the relationship between ion conductivity and surface response kinetics.

The electrolytes used in this study, specifically KOH, Na<sub>2</sub>SO<sub>4</sub>, and their mixture, play a crucial role in influencing the cyclic performance of the electrodes due to their distinct ionic characteristics. The size of the ions, their mobility within the electrolyte, and their chemical interactions with the electrode surface significantly impact the overall electrochemical behaviour. Moreover, the structural and compositional properties of the electrodes themselves, particularly in terms of their material composition and surface morphology, also contribute to the cyclic performance observed. In addition, the applied voltages during the electrochemical deposition process are critical in determining the specific capacitance values achieved. Varying the deposition voltage directly influences the nucleation and growth dynamics of the Mn-Cu film on the graphite substrate. Specifically, the applied growth voltages can significantly influence the deposition rates, the uniformity of the deposited particles, and the resulting surface area available for charge storage. These factors, in turn, play an important role in determining the capacitance, as variations in deposition conditions directly affect the microstructural properties of the electrode surface and its capacity for efficient charge accumulation.

**Table 4.** Comparison of electrode capacitances for supercapacitors as reported in the literature

Electrode Material	Method	Specific Capacitance (mF cm <sup>-2</sup> )	Electrolyte	Reference
MnO <sub>2</sub>	Electrodeposition	13	Na <sub>2</sub> SO <sub>4</sub>	(Tran et al., 2020)
CuO/rGO	Hydrothermal	80	Na <sub>2</sub> SO <sub>4</sub>	(Bu and Huang, 2017)
NiO-TiO <sub>2</sub>	Potentiostatic anodization	46	NaOH	(Xie et al., 2009)
Ni(OH) <sub>2</sub>	Facile hydrothermal	36	PVA-KOH	(Dong et al., 2014)
Mn-Cu	Electrodeposition	109	KOH + Na <sub>2</sub> SO <sub>4</sub>	This work

#### 4. Conclusion

The development of technologies that make use of flexible screens and sensors has seen significant progress in recent years. On the other hand, the development of flexible energy storage technologies has been somewhat slow in comparison to other areas of research. It is essential to do research on flexible energy storage electrodes because of the significant role that flexibility and stretchability play in the development of wearable, biomedical, and portable electrical electronic devices. Within the scope of this research work, the electrochemical properties of graphite filaments that have been coated with an alloy and exhibit flexibility are investigated. The electrochemical synthesis of modified graphite based on manganese and copper was accomplished in a deep eutectic solvent ionic liquid, which altered the static voltage levels. The performance of electrochemical deposition of films in Ethaline deep eutectic solvent was analyzed in this study. The alloy was obtained from Mn and Cu-based chloride salts in an Ethaline ionic liquid. The growth potentials were -1.6, -1.9 and -2.2 V. The subsequent cycling of the resultant electrodes in a KOH, Na<sub>2</sub>SO<sub>4</sub>, and the mixture of KOH and Na<sub>2</sub>SO<sub>4</sub> electrolytes was also analyzed. An increase to 1.5 V was made to the potential window that was utilized for this investigation. It was determined how much the areal capacitance of the flexible electrodes that were manufactured was. It is possible to exert control over the performance of the electrode by modifying the structure of the material through alterations in the conditions under which the deposition takes place. After being coated with Mn-Cu by means of an application of a voltage of -1.9V, the graphite substrate displayed a length capacitance of 109 mF cm<sup>-2</sup> when the cycling electrolyte was a mixture of potassium hydroxide and sodium sulfate. There was a significant amount of surface covering on the film, which indicates that it has the potential to be deployed in energy storage applications.

#### Acknowledgments

The authors thank the Scientific Research Project Unit at Gaziantep University (MF.ALT.22.18).

#### Ethics Permissions

In studies requiring ethics committee permission, information about the permission (committee name, date and issue number) should be given in the method section and also on the last page of the article.

#### Author Contributions

Abdulcabbar Yavuz and Hüseyin Faal contributed to the study's conception and design. Material preparation, data collection, and analysis were performed by Abdulcabbar Yavuz and Hüseyin Faal. The calculations were performed by Hüseyin Faal. Abdulcabbar Yavuz supervised the project. Hüseyin Faal wrote the first draft of the manuscript, and Abdulcabbar Yavuz commented on previous versions of the manuscript. All authors read and approved the final manuscript.

#### Conflict of Interest

Authors declare that there is no conflict of interest for this paper.

#### References

- Arumugam, B., Mayakrishnan, G., Subburayan Manickavasagam, S. K., Kim, S. C., and Vanaraj, R. (2023). An overview of active electrode materials for the efficient high-performance supercapacitor application. *Crystals*, 13(7), 1118.
- Baig, M. M., Khan, M. A., Gul, I. H., Rehman, S. U., Shahid, M., Javaid, S., and Baig, S. M. (2023). A review of advanced electrode materials for supercapacitors: challenges and opportunities. *Journal of Electronic Materials*, 52(9), 5775–5794.
- Brisse, A. L., Stevens, P., Toussaint, G., Crosnier, O., and Brousse, T. (2018). Ni(OH)<sub>2</sub> and NiO based composites: Battery type electrode materials for hybrid supercapacitor devices. *Materials*, 11(7), 1178.
- Bu, I. Y. Y., and Huang, R. (2017). Fabrication of CuO-decorated reduced graphene oxide nanosheets for supercapacitor applications. *Ceramics International*, 43(1), 45–50.
- Dong, X., Guo, Z., Song, Y., Hou, M., Wang, J., Wang, Y., and Xia, Y. (2014). Flexible and wire-shaped micro-supercapacitor based on Ni(OH)<sub>2</sub>-nanowire and ordered mesoporous carbon electrodes. *Advanced Functional Materials*, 24(22), 3405–3412.

- González, A., Goikolea, E., Barrera, J. A., and Mysyk, R. (2016). Review on supercapacitors: Technologies and materials. *Renewable and Sustainable Energy Reviews*, 58, 1189–1206.
- Guney, M. S., and Tepe, Y. (2017). Classification and assessment of energy storage systems. *Renewable and Sustainable Energy Reviews*, 75, 1187–1197.
- Hannan, M. A., Wali, S. B., Ker, P. J., Abd Rahman, M. S., Mansor, M., Ramachandaramurthy, V. K., Muttaqi, K. M., Mahlia, T. M. I., and Dong, Z. Y. (2021). Battery energy-storage system: A review of technologies, optimization objectives, constraints, approaches, and outstanding issues. *Journal of Energy Storage*, 42, 103023.
- Ho, J., Jow, T. R., and Boggs, S. (2010). Historical introduction to capacitor technology. *IEEE Electrical Insulation Magazine*, 26(1), 20–25.
- Iro, Z. S., Subramani, C., and Dash, S. S. (2016). A brief review on electrode materials for supercapacitor. *International Journal of Electrochemical Science*, 11(12), 10628–10643.
- Kalhammer, F. R., and Schneider, T. R. (1976). Energy storage. *Annual Review of Energy*, 1(1), 311–343.
- Li, H. Q., Wang, Y. G., Wang, C. X., and Xia, Y. Y. (2008). A competitive candidate material for aqueous supercapacitors: High surface-area graphite. *Journal of Power Sources*, 185(2), 1557–1562.
- Luo, X., Wang, J., Dooner, M., and Clarke, J. (2015). Overview of current development in electrical energy storage technologies and the application potential in power system operation. *Applied Energy*, 137, 511–536.
- Mitali, J., Dhinakaran, S., and Mohamad, A. A. (2022). Energy storage systems: A review. *Energy Storage and Saving*, 1(3), 166–216.
- Mohanty, R. I., Mukherjee, A., Bhanja, P., and Jena, B. K. (2023). Novel microporous manganese phosphonate-derived metal oxides as prospective cathode materials for superior flexible asymmetric micro-supercapacitor device. *Journal of Energy Storage*, 72, 108730.
- Niknam, E., Naffakh-Moosavy, H., and Afshar, M. G. (2022). Electrochemical performance of nickel foam electrode in potassium hydroxide and sodium sulfate electrolytes for supercapacitor applications. *Journal of Composites and Compounds*, 4(12), 149–152.
- Purushothaman, K. K., Cuba, M., and Muralidharan, G. (2012). Supercapacitor behavior of  $\alpha$ -MnMoO<sub>4</sub> nanorods on different electrolytes. *Materials Research Bulletin*, 47(11), 3348–3351.
- Sahin, M. E., Blaabjerg, F., and Sangwongwanich, A. (2020). A review on supercapacitor materials and developments. *Turkish Journal of Materials*, 5(2), 10–24.
- Sayed, S. G., Shaikh, A. V., Shinde, U. P., Hiremath, P., and Naik, N. (2023). Copper oxide-based high-performance symmetric flexible supercapacitor: Potentiodynamic deposition. *Journal of Materials Science: Materials in Electronics*, 34(17), 1361.
- Sharma, K., Arora, A., and Tripathi, S. K. (2019). Review of supercapacitors: Materials and devices. *Journal of Energy Storage*, 21, 801–825.
- Tran, C. C. H., Santos-Peña, J., and Damas, C. (2020). Electrodeposited manganese oxide supercapacitor microelectrodes with enhanced performance in neutral aqueous electrolyte. *Electrochimica Acta*, 335, 135564.
- Wen, Q., Chen, J. X., Tang, Y. L., Wang, J., and Yang, Z. (2015). Assessing the toxicity and biodegradability of deep eutectic solvents. *Chemosphere*, 132, 63–69.
- Xie, Y., Huang, C., Zhou, L., Liu, Y., and Huang, H. (2009). Supercapacitor application of nickel oxide–titania nanocomposites. *Composites Science and Technology*, 69(13), 2108–2114.
- Yang, Y., Bremner, S., Menictas, C., and Kay, M. (2018). Battery energy storage system size determination in renewable energy systems: A review. *Renewable and Sustainable Energy Reviews*, 91, 109–125.
- Yavuz, A., Artan, M., and Yilmaz, N. F. (2022). The effect of growth potential on the self-discharge behavior of Cu–Ni based alloy electrodes. *Journal of Physics and Chemistry of Solids*, 169, 110872.